CLIMATOLOGICAL CHARACTERISTICS AND OROGRAPHIC ENHANCEMENT OF LAKE-EFFECT PRECIPITATION OVER EASTERN LAKE ONTARIO AND THE TUG HILL PLATEAU

by

Peter Gregory Veals

A thesis submitted to the faculty of
The University of Utah
in partial fulfillment of the requirements for the degree of

Master of Science

Department of Atmospheric Sciences

The University of Utah

December 2014

The University of Utah Graduate School

STATEMENT OF THESIS APPROVAL

The thesis of **Peter Gregory Veals**

has been approved by the following supervisory committee members:

William James Steenburgh	, Chair	**8/13/2014** Date Approved
John D. Horel	, Member	**8/13/2014** Date Approved
Courtenay Strong	, Member	**8/13/2014** Date Approved

and by **Kevin D. Perry**, Chair/Dean of

the Department/College/School of **Atmospheric Sciences**

and by David B. Kieda, Dean of The Graduate School.

ABSTRACT

The Tug Hill Plateau of upstate New York rises approximately 500 m above Lake Ontario, observes frequent (often heavy) lake-effect snowfall, and is one of the snowiest regions in the eastern United States. This work presents a climatology of lake-effect precipitation created using data from the KTYX WSR-88D radar situated atop the plateau. Base reflectivity imagery was manually examined to identify lake-effect periods (LEPs) during each cool season (16 Sep – 15 May) from 16 Sep 2001 – 15 May 2014.

The most active months for lake effect in this region are December and January. There is a tendency for LEPs to begin within a few hours before and after sunset in the spring and fall, with no such diurnal signal observed in the winter. Correspondingly, lake effect is slightly more frequent at night than during the day. Overall, the diurnal variability is weaker than found over smaller bodies of water such as the Great Salt Lake of Utah.

Classification of events by morphological type revealed that broad coverage and long-lake-axis-parallel (LLAP) account for ~72% and ~24% of lake-effect hours, respectively. The diurnal signal for broad coverage (LLAP) events was less (more) pronounced than for LEPs in general.

The near-shore areas south and east of Lake Ontario receive the most frequent lake-effect precipitation. The Tug Hill Plateau produces a strong orographic signal, with an echo frequency maximum on the western (typically windward) slope. Data from cooperative observer (COOP) sites and the Snow Data Assimilation System (SNODAS)

corroborate these radar-derived results. The 'broadening' of high echo frequency over the Tug Hill Plateau, as well as the existence of the lake-orographic morphology, may point to inland/orographic intensification and generation of precipitation during some LEPs.

TABLE OF CONTENTS

ABSTRACT iii

ACKNOWLEDGEMENTS vi

Chapters

1. INTRODUCTION 1

    1.1 Lake Effect in the Great Lakes and Tug Hill Region 1
    1.2 Morphological Classification 2
    1.3 Regional Variation and Orographic Effects on Lake-Effect Precipitation 4
    1.4 Summary 6

2. DATA AND METHODS 8

    2.1 Event Identification and Morphological Classification 8
    2.2 Radar Capabilities, Limitations, and Statistics 10
    2.3 Additional Datasets 11

3. RESULTS 13

    3.1 LEP Characteristics and Intraseasonal Variability 13
    3.2 Interannual Variability and Contributions to Hydroclimate 14
    3.3 Diurnal Variability 16
    3.4 Spatial Characteristics Derived from Radar 18
    3.5 Morphological Characteristics 23

4. SUMMARY AND CONCLUSION 40

    4.1 Summary of Findings 40
    4.2 Conclusion and Future Work 42

REFERENCES 44

ACKNOWLEDGEMENTS

I would like to acknowledge my amazing family for all the love, support, and encouragement they have given me, and my friends who have kept me sane throughout the trials of the graduate school process. My fellow graduate students, especially those in the Mountain Meteorology Group, have provided invaluable assistance in this research. My advisor, Dr. Jim Steenburgh, has been a constant source of mentoring, inspiration, patience, and enthusiasm. I would also like to thank Drs. John Horel and Courtenay Strong for putting in the time and effort to improve this thesis as members of my committee. Carol Yerdon, of North Redfield, NY, also provided an impeccable 19-year record of snowfall observations that proved to be a great addition to this paper, and other data were graciously provided by the National Operational Hydrologic Remote Sensing Center and the National Climatic Data Center. Funding for this project from the National Science Foundation under grants AGS-0938611 and AGS-1262090 and from the NOAA/National Weather Service C-STAR program under NA13NWS5680003. Any opinions, findings, conclusions, or recommendations expressed are those of the authors and do not necessarily reflect those of the National Science Foundation or the NOAA/National Weather Service.

CHAPTER 1

INTRODUCTION

1.1 Lake Effect in the Great Lakes and Tug Hill Region

The Great Lakes of North America produce frequent, sometimes intense, lake-effect snowstorms during the cool season (e.g., Niziol et al. 1995). High snowfall rates, low visibility, and heavy accumulations impact commerce and transportation, but also contribute to a vibrant winter-sports economy (Tug Hill Commission 2014). The area to the east of Lake Ontario in particular observes some of the most intense snowstorms in the world, many enhanced over the Tug Hill Plateau, which rises ~500 m above lake level. World record snowfall accumulations observed in this region include 30.5 cm (12 in) in 1 h at Copenhagen, NY, 44.5 cm (17.5 in) in 2 h at Oswego, NY, and 129.5 cm (51 in) in 16 h at Bennetts Bridge, NY (Burt 2007). An observer in Montague, NY reported a 24-h snowfall of 195.6cm (77in), but is not recognized as an official record since 6 measurements were taken during the period instead of 4 (Leffler et al. 1997). Much of the Tug Hill Plateau averages over 500 cm (200 in) of snow per year, with a record 1173cm (462 in) observed in Hooker during the 1976–77 cool season.

Lake effect occurs when cold air passing over a warm body of water gains enough latent and sensible heat to trigger moist convection, conditions that are frequently present in the Great Lakes region (e.g., Dole 1928; Peace and Sykes 1966; Niziol et al. 1995). Most wintertime (December, January, and February) lake-effect precipitation in the Great

Lakes region falls in the form of snow, although fall (September, October, and November) events sometimes produce rain, especially prior to early November (Miner and Fritsch 1997). Lake-effect snowfall accumulations increase through the fall over the Great Lakes, peak in early winter, and then decrease as the lakes cool and, in some winters, become partially or fully ice covered (Niziol et al. 1995). Kristovich et al. (2005) suggest that the frequency of lake-effect precipitation in the Great Lakes region is highest in the overnight/early morning hours and lowest in the afternoon. Similar diurnal modulation of lake-effect frequency has also been documented over the Great Salt Lake of Utah, especially in the spring [March, April, and May (Steenburgh et al. 2000; Alcott et al. 2012)].

1.2 Morphological Classification

Synoptic, mesoscale, lake-surface, and land-surface conditions influence the area, intensity, and organization of lake-effect precipitation systems, leading to a rich morphological spectrum that includes:

1) Wind-parallel bands that are usually generated by land-breeze-induced convergence and typically form when the prevailing flow is oriented along the long axis of an elongated body of water such as Lake Michigan, Lake Erie, Lake Ontario, or the Great Salt Lake (e.g., Peace and Sykes 1966; Passarelli and Braham 1981; Braham 1983; Hjelmfelt 1990; Niziol et al. 1995; Steenburgh et al. 2000; Alcott et al. 2012). Sometimes called midlake or shoreline bands (Laird and Kristovich 2004), following Steiger et al. (2013), we will refer to this morphological regime as *long-lake-axis-parallel (LLAP) bands*. LLAP bands can extend well inland and typically produce the most intense snowfall rates and heaviest accumulations (Niziol et al. 1995; Steiger et al. 2013).

2) *Broad coverage* events that typically feature open-cellular convection or multiple, quasi-periodic wind-parallel bands produced by horizontal roll convection (e.g., Kelly 1982, 1984, 1986; Kristovich 1993; Laird and Kristovich 2004).

3) *Hybrid events* that have characteristics of LLAP bands and broad coverage events. This morphological regime is synonymous with the hybrid classification of Niziol et al. (1995), who referred to LLAP band and broad coverage events as Type I and II, respectively. In some instances, the LLAP band may form over an upstream lake and merge with broad coverage over a downstream lake. Although it is possible to have hybrids of other morphological regimes, this is the most common.

4) *Shoreline bands*, forming in cold, relatively calm conditions commonly found near the center of winter anticyclones. They are initiated by land-breeze convergence, form and remain close to the shoreline, and exhibit little movement due to weak flow (e.g., Kelly 1986; Hjelmfelt 1990; Niziol et al. 1995). In this study, we distinguish shoreline bands from LLAP bands by requiring the former to penetrate no more than 20 km inland and feature slow or nonexistent movement of cells within the band. Though others such as Laird and Kristovich (2004) have opted to merge shoreline and LLAP bands into a single category, we maintain a separate category, as shoreline bands exhibit different characteristics than LLAP bands, especially for orographic enhancement.

5) *Mesoscale vortices* that form most frequently during weak flow, often where the lakeshore has a bowl-shaped configuration (Forbes and Merritt 1984; Niziol et al. 1995; Laird 1999).

1.3 Regional Variation and Orographic Effects on Lake-Effect Precipitation

Lake-effect precipitation has been the subject of much research over the past 50 years, and while the Great Lakes of North America have received considerable attention, lake effect does occur in other parts of the world. The cold, persistent flow across the Sea of Japan during the Asian Winter Monsoon produces heavy snow accumulations on the densely populated Japanese Islands (e.g., Magono 1966; Hozumi 1984; Matsuura et al. 2005). At an elevation of 2 m MSL, the city of Aomori near the northern end of Honshu Island has a population of 300,000 and a mean annual snowfall of 775 cm (Steenburgh 2014). Lake-effect snow from the Black Sea has paralyzed the city of Istanbul, Turkey (Kindap 2010). Even the relatively small Great Salt Lake of Utah produces episodes of lake-effect snow each season, occasionally with accumulations in excess of 50 cm (e.g., Carpenter 1993; Steenburgh et al. 2000; Steenburgh 2003; Alcott et al. 2012).

Within many of the lake-effect prone areas of the world there exists the compounding influence of orography. Japan's Honshu and Hokkaido Islands feature numerous mountains over 1500 m MSL (some over 3000 m MSL) that frequently observe heavy snowfall (Matsuura et al. 2005). There are, however, significant variations in lowland and mountain snowfall during individual storms depending on the height of the "capping" inversion, which affects the depth of the snow-producing clouds. During shallow storms, snow accumulations can be greater in the Japanese lowlands than the high mountains. Magono et al. (1966) refer to these as *Satoyuki* (lowland) storms and events with heavier mountain accumulations as a *Yamayuki* (mountain) storms.

Northern Utah is another region where lake-effect precipitation interacts with

complex terrain, with mountains surrounding the Great Salt Lake reaching up to 2300 m above lake level (Steenburgh et al. 2000; Steenburgh and Onton 2001; Onton and Steenburgh 2001; Alcott et al. 2012; Yeager et al. 2013). Alcott and Steenburgh (2013) showed that the influence of mountains during a Great Salt Lake effect event was multifaceted. Upstream terrain forced a drying, foehn-like flow that was detrimental to lake effect, whereas the concave shape created by topography downstream of the lake reinforced the lake-breeze-induced convergence zone, greatly enhancing the storm intensity. Where the lake band impinged on the high terrain of the Wasatch Mountains, precipitation totals were ~6 times greater than those observed near the shore of the lake. Climatological analysis by Yeager et al. (2013) shows a factor of four increase in mean precipitation produced during lake-effect periods from the lowlands to the mountains southeast of the Great Salt Lake.

Although the terrain is more modest than that of Japan or Utah, orography does influence lake-effect precipitation in the Great Lakes region. As noted by Niziol et al. (1995), "the greatest snowfall occurs where the prevailing winds blow across the longest fetch of the lake, particularly where orographic features enhance precipitation processes." Muller (1966) found a 36–60 cm increase in mean annual snowfall per 100 m increase in elevation in the Great Lakes snowbelts, whereas Hill (1971) found a 25–50 cm increase per 100 m east of Lakes Erie and Ontario. Using numerical simulations, Hjelmfelt (1992) showed that even the minor terrain downstream of Lake Michigan can enhance lake-effect precipitation.

The Tug Hill Plateau rises to 500 m above Lake Ontario over a horizontal distance of ~40km, a remarkably gradual mean slope of only 1.25% (Fig. 1). Mean

September–May precipitation based on National Weather Service Cooperative Observer (COOP) data (1994–2014) increases from 83.7 cm (33.0 in) at Watertown [WTN (151 m MSL)] just north of the plateau to 109 cm (42.9 in) at HKR (448 m MSL) on the plateau (see Fig. 1 for locations). Snowfall increases from 288 cm (113 in) at WTN to 571 cm (225 in) at HKR, although, as will be shown later, these sites are not well situated to identify the orographic precipitation gradient on the western slope or the area of heaviest snowfall on the plateau. In addition to weather impacts, precipitation and snowfall enhancement over the Tug Hill Plateau affects water availability and hydroelectric power generation (Norton and Bolsenga 1993), as well as spatial patterns of forests and other ecological systems (e.g., Henne et al. 2007).

1.4 Summary

In this study, we develop a radar-based climatology to provide new insights into the characteristics and orographic enhancement of lake-effect precipitation east of Lake Ontario and over the Tug Hill Plateau. Chapter 2 describes the data and methods used, including the approaches for the manual identification and morphological classification of lake-effect events. Chapter 3 details intraseasonal variability, interannual variability, contributions to hydroclimate, diurnal variability, spatial characteristics, and morphological characteristics of lake-effect events, with emphasis on environmental factors and the influence of the Tug Hill Plateau. These findings are potentially beneficial to advancing the understanding of lake-effect processes, orographic precipitation enhancement, and the hydroclimate of the region. Discussion and conclusions are presented in Chapter 4.

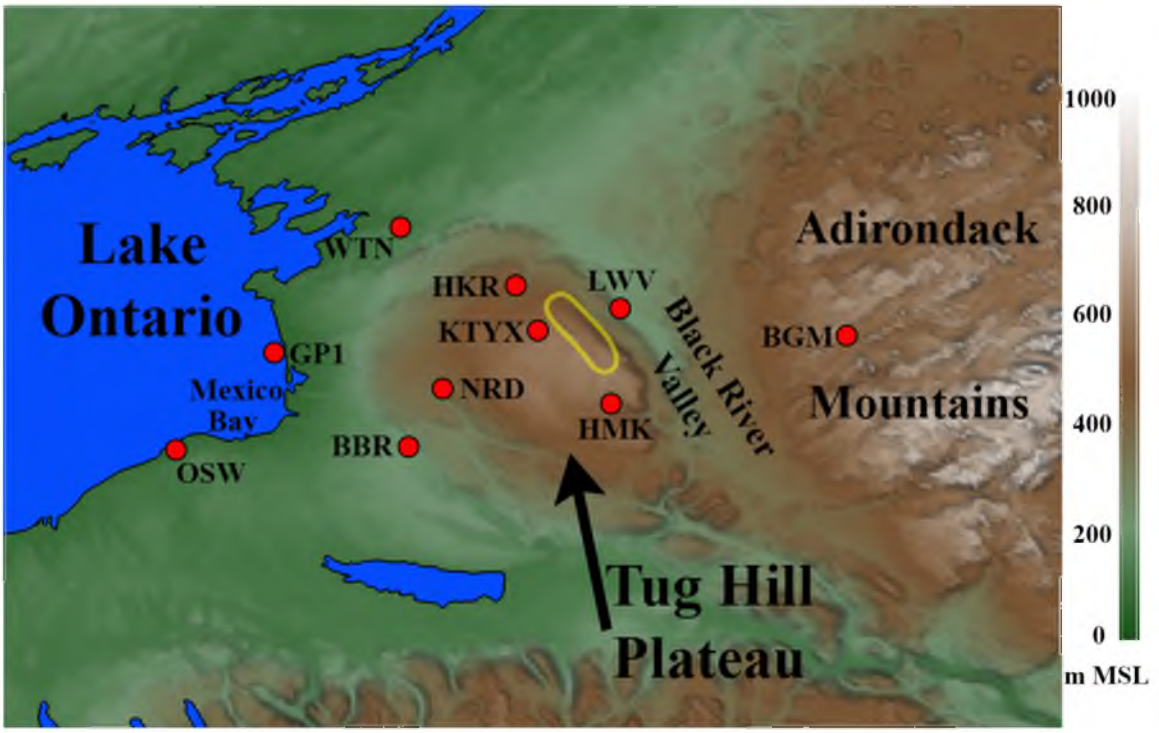

Figure 1: Topographic and geographic features of the study region. Abbreviations include BBR (Bennetts Bridge COOP site), BGM (Big Moose 3SE COOP site), GP1 (NARR grid point for conditional climatologies), HKR (Hooker 12NNW COOP site), HMK (Highmarket COOP site), KTYX (WSR-88D radar), LWV (Lowville COOP site), NRD (North Redfield snow observer), OSW (Oswego East COOP site), and WTN (Watertown COOP site). The yellow line circumscribes the Maple Ridge Wind Farm.

CHAPTER 2

DATA AND METHODS

2.1 Event Identification and Morphological Classification

Lake-effect periods (LEPs) were identified visually using all available lowest-elevation tilt (0.5°) base reflectivity imagery from the KTYX WSR-88D radar during the cool season (16 September – 15 May) from 16 September 2001–15 May 2014. Radar data were obtained from the National Climatic Data Center Hierarchical Data Storage System in level III format (Crum et al. 1993). Data were missing for 4.3% of the study period.

Following Laird et al. (2009a) and Alcott et al. (2012), LEPs were identified as periods $\geq$ 2 h during which precipitation features were: 1) coherent and quasi-stationary with a distinct connection to the lake; 2) shallow and distinguishable from large transitory synoptic features; 3) exhibiting increasing depth and/or intensity in the downwind direction. This definition includes periods when lake-effect precipitation features occur concurrently with synoptically forced and other non-lake-effect precipitation. The $\geq$ 2 h duration is longer than the $\geq$ 1 h used by Alcott et al. (2012) for the Great Salt Lake. Although lake-effect identification was frequently straightforward, we consulted surface observations, upper air soundings, and satellite images from the UCAR MMM Image Archive when event identification was ambiguous based on radar alone.

Although the manual identification process is to some degree inherently

subjective, the criteria listed above were adhered to in order to make the process as objective as possible. There were a handful of cases that appeared ambiguous and were difficult to categorize, but these were generally short-lived and have little effect on the overall statistics. It would be possible to perform an event identification using a machine learning algorithm, but we felt that there would be too many missed events and false alarms. Such an algorithm could be successful, however, and would have to take into account as many of the characteristics that are noticed by the human observer as possible. For example, it would need to be able to recognize the appearance of individual cells propagating within an organized, quasi-stationary band, or cells generating over the lake in the same position and moving downstream (but not having a connection to a larger-scale, non-lake-effect convective system).

The morphology of lake-effect features was also identified based on the categories described in the introduction [i.e., *LLAP* (usually 1 but in some cases 2 bands), *broad coverage*, *hybrid*, *shoreline*, and *mesoscale vortex*], plus *lake–orographic* and *miscellaneous* (no clear fit into any of the aforementioned categories). The lake-orographic category featured a stationary precipitation area confined to the plateau with only weak or intermittent lake-effect features developing over the lake during the period encapsulating the orographic precipitation.

Start and end times for the existence of a morphological category were recorded, with persistence $\geq$ 1 h required for inclusion. Two or more morphological types were noted in instances where they occurred concurrently. For example, LLAP bands sometimes occurred concurrently with broad coverage. Example base reflectivity images of each morphology type are shown in Fig. 2.

2.2 Radar Capabilities, Limitations, and Statistics

The KTYX radar is located at 562 m MSL on the Tug Hill Plateau (Fig. 1). The fairly continuous data availability over the 13 cool seasons of the study period, combined with the proximity to and view over the plateau and eastern shore of Lake Ontario, allows for a unique spatial perspective of lake effect precipitation in the region. Nevertheless, some problems are caused by the Maple Ridge Wind Farm along the eastern side of the plateau (Fig. 1), which leads to reduced down-radial signal power and produces multi-path/interturbine scattering, multitrip echoes, and spurious high reflectivity values (Radar Operations Center 2010; NWS 2012). This affects radar returns in the wind farm area and down-radial areas over the Black River Valley and western Adirondack Mountains (see Fig. 1 for locations), as discussed where necessary later in the analysis. Unrelated to the wind farm and depending on stability, there are occasionally blocked radials or clutter removal along the ~135° and ~340° azimuths.

Bragg scattering was observed near the radar during a small number of LEPs. We elected not to remove these events since they were infrequent and thus have minimal impact on results. Finally, although beam height is low enough to detect precipitation falling over and near the Tug Hill Plateau, lake-effect convection is sometimes confined to below 2 km MSL, and the centroid of the 0.5° scan reaches this altitude at about 100-km range (Fig. 3). Therefore, lake-effect features may go undetected or only partially fill the beam at longer ranges (Brown 2007). In addition, low-level hydrometeor growth or sublimation may be undetected.

Spatial statistics were generated using the 0.5° base reflectivity scans to better understand the distribution and intensity of precipitation during the LEPs. Although the

time between volume scans can vary from 5–12 min due to changes in radar scan mode, no attempt was made to apply a time-weighting algorithm because the events with longer-interval scans typically feature weaker, less persistent echoes and are generally underrepresented without time-weighting.

2.3 Additional Datasets

Conditional radar statistics were generated using data from the North American Regional Reanalysis (NARR; Mesinger et al. 2006), which were obtained from the National Climatic Data Center (NCDC). Specifically, we used data from a NARR grid box centered at 43.7°N and 76.2°W (GP1 in Fig. 1), ~2.5 km upstream of the eastern shore. Although the use of reanalysis data has its limitations, low frequency, remoteness, and questionable representativeness precludes the use of upper-air observations from the nearest regular sounding sites in Buffalo and Albany, NY. Snow depth and snowpack water content analyses were obtained from the National Operational Hydrologic Remote Sensing Center (NOHRSC) Snow Data Assimilation System (SNODAS; National Operational Hydrologic Remote Sensing Center 2004). SNODAS uses RUC/RAP snowfall analysis data, ground observations, data from airborne platforms, and space-borne microwave remote sensing to estimate snow depth and snowpack snow water equivalent (SWE) at 1-km spatial and 24-h temporal resolution. Daily and climatological averages for COOP stations were obtained from NCDC. In addition, we obtained a temporally complete 19-year record of snowfall observations from a National Weather Service spotter at North Redfield (labeled NRD in Fig. 1) that is not included in the NCDC COOP records.

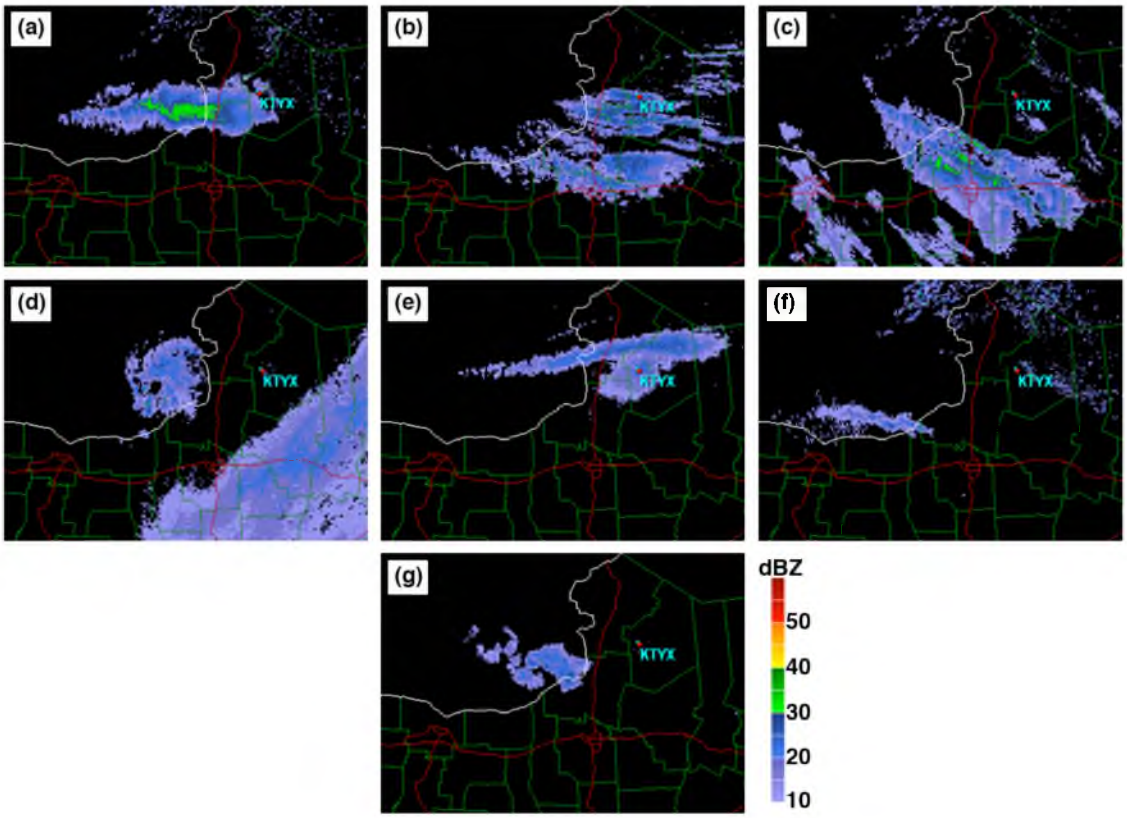

Figure 2. Lowest-tilt (0.5°) base reflectivity examples of lake-effect morphological types: (a) LLAP, (b) broad coverage, (c) hybrid, (d) mesoscale vortex, (e) lake–orographic (concurrent with LLAP band to north), (f) shoreline, and (g) miscellaneous.

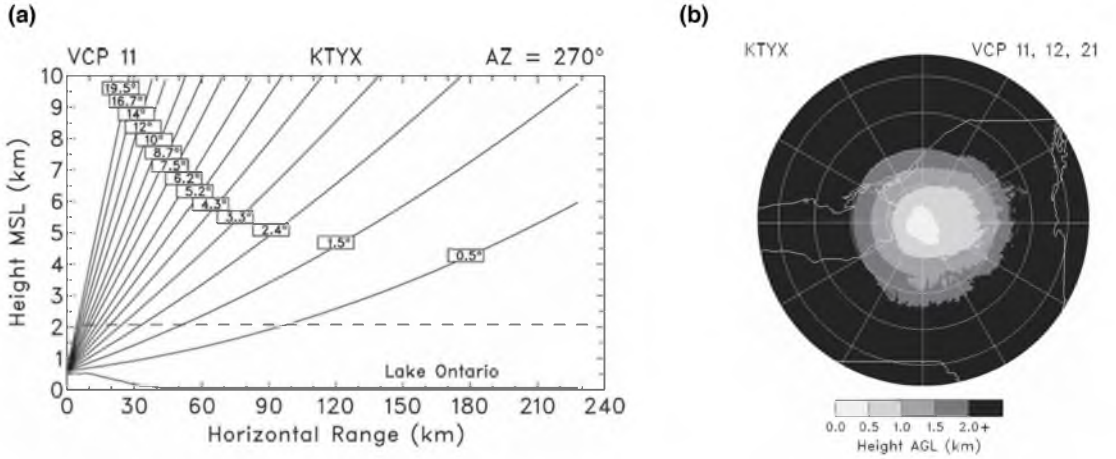

Figure 3. (a) Height of the KTYX beam centroids at various elevation angles. (b) Height of the KTYX 0.5° beam centroid above ground level. Adapted from Brown (2007). Copyright American Meteorological Society.

CHAPTER 3

RESULTS

3.1 LEP Characteristics and Intraseasonal Variability

A total of 636 LEPs were identified during the 13 cool season study period. The mean (median) LEP duration was 19.5 h (13.2 h), with the longest event lasting 237 h (9.9 d; 3–12 Feb 2007) and producing 358 cm (141 in) of snow in North Redfield (NRD; see Fig. 1 for location) on the western slope of the plateau (NWS 2007). Although short LEPs are the most common, with the frequency decreasing with duration, there were 42 that lasted $\geq$ 48 h, yielding a mean of 3.2 per cool season (Fig. 4).

The most active month for lake effect was January, with 2862 h (29.5% of the time), followed closely by December (29.4% of the time; Fig. 5). May was the least active month, with 2 LEPs observed, accounting for 0.6% of the time. The decreasing lake-effect frequency from January through the end of the cool season is generally attributed to decreasing lake-surface temperatures and increasing air temperatures (e.g., Niziol et al. 1995). Lake Ontario rarely develops significant ice cover, so freezing of the lake is not likely a major factor in the decrease, although the freezing of upstream lakes could have some influence. This seasonal cycle contrasts with that found over the Great Salt Lake of Utah where lake effect frequency features a bimodal distribution with peaks in the fall and spring (Alcott et al. 2012). This reflects the shallow (3 m average depth), hypersaline composition of the Great Salt Lake, which prevents freezing and leads to

rapid warming in the spring, in contrast to the deeper, freshwater Lake Ontario.

3.2 Interannual Variability and Contributions to Hydroclimate

The occurrence of lake effect varied from 577 h during the 2012 cool season (defined based on the ending calendar year) to 1308 h during the 2007 cool season (Fig. 6), with a mean of 956 and standard deviation of 177. The 2007 cool season also featured the aforementioned 237 h LEP. The number of LEPs per cool season ranged from 41 to 66. Alcott et al. (2012) documented a larger interannual variability in Great Salt Lake effect, with cool seasons experiencing anywhere from 3 to 20 LEPs.

The hours of lake effect, however, do not account for coverage and intensity, which ultimately play an important role in the snow climate of the region. Therefore, data from available COOP observer sites and the North Redfield spotter site were analyzed for the 13 cool season study period to provide insight into the total snowfall and snow water equivalent (SWE; the liquid equivalent of any precipitation) across the study region and to estimate the lake-effect fraction (LEF), the fraction of snow or SWE generated on lake-effect days (LEDs; defined as having $\geq$ 2 h of lake-effect). Estimating the LEF involved partitioning the daily (0800–0800 EST for the COOP sites and 0000–0000 EST for North Redfield) snowfall and SWE into LEDs and non-LEDs. Although some non-lake-effect snow and SWE may have fallen on these LEDs, this approach provides a rough estimation of the significance of lake-effect precipitation to the region.

Total cool-season snowfall (i.e., that produced on LEDs and non-LEDs) is significantly greater over the plateau compared to lowland sites (Table 1; Fig. 7). The 2 sites over 400 m MSL (HKR and HMK) have a mean cool-season snowfall > 500 cm and SWE > 110 cm, whereas the Watertown (WTN) site at 152m MSL observes 304 cm and

88 cm, respectively. Furthermore, on the western slope of the plateau, NRD (399 m MSL) observes a mean cool-season snowfall of 718 cm, the highest of any site in the area (SWE data not available). As shown later, the greater snowfall at NRD agrees well with spatial radar statistics, which place the area of greatest snowfall on the western slope of the plateau near NRD and intermediate to HKR and HMK.

The LEF for cool-season snowfall is greater than .47 for all sites and cool seasons and reaches as high as .90 during the 2002 cool season at HMK and 2013 cool season at NRD (Fig. 7). Over the study period, the mean LEF at near-lake and plateau sites exceeds .70, with a lesser, but still sizeable mean LEF of .61 at Big Moose 3SE (BGM) in the Adirondacks (Table 1). These values indicate that lake effect is the dominant production mechanism for snowfall in the region. The LEFs for cool-season SWE, however, are considerably lower than those for snowfall, ranging from .13 at BGM during the 2013 cool season to .63 at HKR during the 2009 cool season (Fig. 8). The HMK, BBR, and HKR sites on the plateau receive the greatest contribution, with mean LEFs for cool-season SWE of .38, .37, and .42, respectively (Fig 8; Table 1).

The LEF for monthly snowfall is highest in the fall and lowest in the spring (Fig. 9). Nearly all of the snow in October and November falls on LEDs, which is plausible given that anomalously cold air is needed to generate snow instead of rain during that time of year and lake-effect is typically generated during such cold-air intrusions. In contrast, during the spring, the LEF is lower as lake effect becomes less frequent and synoptic systems dominate the snowfall accumulations. The LEF for SWE peaks in December and January instead of October and November, likely due to the large amounts of non-lake-effect rain observed in September and October (Fig. 10). One notable non-

lake-effect contribution during the study period came from the remnants of Tropical Storm Nicole, which brought widespread rainfall amounts >7 cm to the region on 1 October 2010.

The larger LEF for snowfall reflects at least two factors. First, due to the thermodynamic profiles typical of lake-effect events, lake-effect snow is typically of low density, with water contents often <6% (Baxter et al. 2005), so the snowfall contribution from these events is prodigious for a given SWE amount. Second, the study region experiences regular synoptic rain events throughout the cool season (including mid winter), which dilutes the lake effect contribution to SWE. Nonetheless, the fact that in some seasons, >50% of the cool-season SWE falls on LEDs at locations like HKR and Bennett's Bridge (BBR), much in the form of snow, shows the importance of lake effect for the regional hydroclimate. The drainage from the Tug Hill Plateau contributes to flows in the Salmon, Black, and Mohawk Rivers, with significance for Atlantic salmon habitat, hydropower generation, and transportation along the New York State Canal System.

3.3 Diurnal Variability

For spring and fall, there is a tendency for lake effect to initiate near/after sunset (Figs. 11a,c) that is significant at the 95% level, but this trend is absent for winter events (Fig. 11b). For the dissipation time, there is little signal in either the spring or winter (Figs. 11e,f), with only fall showing a tendency for events to end near or following sunrise (significant at the 95% level, Fig. 11d). Overall, the number of days with lake-effect at a given time of day shows a weak, broad minimum in the afternoon hours [~1800–2300 UTC (1300–1800 EST)] and a weak, broad maximum overnight [~0400–

0800 UTC (2300–0300 EST)] in the fall and spring, both of which are significant at the 95% level (Figs. 12a,b). There is no significant signal (at the 95% level) during the winter (Fig. 12c). Statistical significance was determined by permutation resampling, which involves generating a synthetic distribution of the mean (Wilks 2006). If a group of bins fell below 95% of this distribution, it could be said that these values were significantly different than the mean value (the null hypothesis can be rejected) at the 95% confidence level.

Previous work from Kristovich and Spinar (2005) describes a similar afternoon minimum and overnight maximum in precipitation on lake-effect days over Lakes Superior and Michigan. They define a lake-effect day (0000–0000 EST) based on the presence of lake-effect features in visible satellite imagery during the illuminated portion of the day, with hourly precipitation data used to examine the diurnal cycle. Their diurnal signal appears to be stronger than found in our radar-based analysis. Our method, however, simply requires the presence of lake-effect precipitation structures, with no requirement for accumulation, so our findings are not equivalent. Alcott et al. (2012) found a pronounced late night/early morning maximum and afternoon minimum over the Great Salt Lake, with the strongest diurnal variation in the spring and weakest in the fall. Collectively, these results suggest that the diurnal modulation of lake-effect occurrence is weakest during the winter and may be strongest during the fall or spring, especially for smaller bodies of water like the Great Salt Lake. Interestingly, Miner and Fritsch (1997) found that lake-effect precipitation was actually more intense in the afternoon and early evening during autumn lake effect rain events. Their lake-effect definition, however, was very broad and included any persistent ($\geq$ 6h) echoes occurring with lower-tropospheric

cold advection within a 400x400 km box centered on Buffalo, NY.

As discussed by Kristovich and Spinar (2005), a variety of factors may be responsible for this diurnal modulation, but they point to the sensible heat flux maximum (largely caused by a maximum in lake-air temperature difference) in the early morning hours as likely being the dominant mechanism. Other studies have also pointed to this as a possible cause (e.g., Hjelmfelt 1990). On the other hand, the diurnal modulation of land-breeze circulations and the afternoon decline in relative humidity accompanying mixed-layer growth have been suggested as contributors over the Great Salt Lake (e.g., Steenburgh et al. 2000; Alcott et al. 2012). The prevailing atmospheric conditions over eastern Lake Ontario are often quite different, however, than those over the Great Salt Lake. The eastern U.S. observes higher relative humidities on an annual mean basis than Utah, many lake-effect events on Lake Ontario feature an airflow and boundary layer that have been modified by upstream lakes (e.g., Rodriguez et al. 2007), and Lake Ontario is much larger, enabling a greater modification of airmasses compared to the Great Salt Lake. Further work is needed to fully understand the diurnal modulation of lake effect and its variability across differing climates and water bodies.

3.4 Spatial Characteristics Derived from Radar

Radar echoes $\geq$ 10 dBZ during LEPs are most frequently located over the western slope of the Tug Hill Plateau, with an arm of locally high frequencies extending to the southeast shore of Lake Ontario near Mexico Bay (Fig. 13a). The frequency of reflectivities $\geq$ 30 dBZ, which reflects the most intense lake-effect precipitation, features a similar pattern (Fig. 13b). As discussed later, the arm that extends to the southeast shore of Lake Ontario reflects the high frequency of LLAP events near Mexico Bay. At

both ≥ 10 and ≥ 30 dBZ, the Maple Ridge Wind Farm produces nonmeteorologically high frequencies over the eastern plateau. In addition, the blocking of radials in the vicinity of the 135° and 340° azimuths results in unrealistically low frequencies [especially at ≥ 30 dBZ (Fig. 13b)] over the crest of the plateau. HKR and HMK, which have mean cool-season LEP snowfalls of 439 cm and 413 cm, respectively, fall within these problematic azimuths. For comparison, NRD on the western slope and near the highest frequency of echoes ≥ 10 and ≥ 30 dBZ, has a cool-season LEP mean of 539 cm (Table 1 and Figs. 13 a,b). Collectively, these results suggest that the maximum in lake-effect precipitation and snowfall likely lies on the western slope or upper plateau near and east of NRD and intermediate to HKR and HMK.

The frequency of echoes ≥ 10 dBZ decreases sharply over the lee slope of the plateau, reaching a minimum over the Black River Valley, and then increasing over the western Adirondack Mountains. Frequencies are lower over the Adirondack Mountains than over the plateau, although multipath scattering and multitrip echoes from the Maple Ridge Wind Farm produce some spurious high values (Fig. 13a). The frequency of radar echoes ≥ 30 dBZ is very low over most of the western Adirondack Mountains, implying that intense lake-effect echoes are rare in this region, although this may reflect partial filling of the radar beam at longer ranges due to overshooting (Fig. 13b).

Given the significant fraction of regional snowfall produced during LEPs, the mean maximum snowpack water content from SNODAS (hereafter simply water content) generally exhibits a spatial pattern similar to the above radar-based analysis (cf. Figs. 13, 14). High water contents are found over the Tug Hill Plateau, with an extension of locally high values along the southeast shore of Lake Ontario near Mexico Bay. Further

east, a minimum is found over the Black River Valley. Water contents over the western Adirondack Mountains, however, are comparable to those found on the plateau, in contrast to the frequencies of radar echoes ≥ 10 and ≥ 30 dBZ, which are much lower. It is possible that overshooting and blockage by the Maple Ridge Wind Farm causes lake effect to be poorly sampled over the western Adirondacks, or that the greater snowpack water contents reflect a larger contribution of non-lake-effect events (especially over the southwest Adirondacks). The latter is considered most likely, as the mean cool-season snowfall for LEPs of 216 cm from the BGM site is the lowest of all the COOP sites in the region (cf. Figs. 13, 14).

The frequency of echoes ≥ 10 dBZ was subdivided based on the mean 975–850 hPa wind direction at the NARR grid point along the east shore of Lake Ontario (see Fig. 1 for location). Frequencies calculated for each subdivision are relative only to that subdivision, not relative to LEPs as a whole. For flows from 240°–249° and 250°–259°, the northern and central plateau observe the highest echo frequencies, but high values extend well into the lee of the plateau to the northwest Adirondacks (Fig. 15a,b). By comparison, for flows from 260°–269° (270°–279°), the central (central and southern) plateau is favored, but the echo frequency decreases more abruptly over the lee slope, with lower values over the Black River Valley and western Adirondacks (Fig. 15c,d). The lower values over the Black River Valley and western Adirondacks may party reflect beam blockage by the Maple Ridge Wind Farm, as discussed previously, and overshooting may affect frequencies over the western Adirondacks.

As the flow veers from 240°–249° to 270°–279°, contributions from LLAP events become more substantial, leading to an increasingly prominent narrow area of high

frequency over southeast Lake Ontario and the adjoining lowlands (Fig. 15a–d). As the flow veers further to 280°–289° and 290°–299°, however, echo frequencies weaken, indicating less intense (having more diffuse echoes) LEPs, with the maximum shifted to lowland areas downstream of the southeast shore of Lake Ontario (Fig. 15e,f).

For most flow directions, but especially those from 260°–269° and 270°–279°, there is a clear broadening of the echo frequency maximum over the Tug Hill Plateau. Thus, precipitation over the plateau tends to not only be more steady with fewer breaks during LEPs, but also more extensive geographically. For example, a LLAP band may broaden over the plateau or be accompanied by an area of orographic precipitation to the north or south. In some LEPs, the lake-orographic morphology dominates, and echo coverage and frequency increase dramatically over the plateau.

Contoured frequency by distance diagrams (CFDD) of radar reflectivity along zonal transects crossing the plateau further highlight the lake and orographic influences during LEPs (Fig. 16). The southernmost plateau transect, X_S, exhibits an increase in reflectivity frequency at all intensities from Lake Ontario to the western slope of the plateau (Fig. 16a). A broad maximum for all intensities extends from the western slope across the upper plateau, with an abrupt decline over the lee slopes to a minimum over the Black River Valley. A secondary maximum lies over the Adirondacks. Although these results are generally consistent with the earlier analysis of observed snowfall and SWE observations, echo frequencies are likely affected by occasional blockage and clutter removal over the upper plateau and by spurious returns produced by the Maple Ridge Wind Farm from the upper plateau to the Adirondacks. The influence of the latter is clearly evident in Fig. 16.

The transect across the center of the plateau, X_c, features an increase in reflectivity frequency at intensities > ~5 dBZ from Lake Ontario to the lower western slope of the plateau, but higher values are eventually achieved over the upper western slope (Fig. 16b). NRD, the snowiest observing site with 718 cm, lies very near the maximum. Curiously, there is a weak minimum of echo frequencies < ~5 dBZ over the western slope, which may indicate a decline in precipitation intermittency in this region during LEPs (i.e., precipitation tends to be steadier with fewer breaks). The Maple Ridge Wind Farm has a stronger influence along this transect, causing spurious returns over the eastern edge of the plateau, so although there is some suggestion of a decline in echo frequency at all intensities before the absolute crest of the plateau is reached, beam blockage and clutter removal affect results in this region.

Echo frequencies at all intensities along the northernmost transect, X_n, are lower than along X_s and X_c over Lake Ontario and the plateau, consistent with the lower frequency of lake effect in this region (Fig. 16c). Structurally, the patterns are, however, similar to those in X_s and X_c. Curiously, although the frequency of echoes > ~10 dBZ is lower over the Adirondacks than the plateau, the frequency of echoes < ~10 dBZ is higher. This could indicate a shift from more intense to less intense echoes as one moves downstream, although issues related to beam overshooting and the effects of the Maple Ridge Wind Farm complicate the analysis.

Meridional CFDD transects were also calculated across the study region (Fig. 17). The westernmost transect, Y_w, lies roughly along the eastern Lake Ontario shoreline near its center, crossing inland at Mexico Bay. The peak in frequency along this transect is located near and just south (inland) of the southern Mexico Bay shoreline (at ~43.5N).

Moving east to transect Y_c, which crosses the western slope of the plateau, the peak in frequency (mainly for low and moderate reflectivity values) lies further north for the Y_c transect than it does for Y_w. This far east of the lake, the signature from the frequent low intensity events affecting the southern Tug Hill is overtaken by the more prevalent and intense echoes generated further north over the west-central slopes of the plateau. The northward shift of the peak frequencies is even more apparent in the Y_e transect, which crosses the high slopes of the plateau. Another feature, most notable along the Y_c transect but possibly present in Y_e, is the decrease in frequency of low intensity echoes over the plateau. As noted previously for the zonal transects, this may reflect a decrease in precipitation intermittency over the plateau compared to the lowlands.

3.5 Morphological Characteristics

Using the morphological classification scheme described in Chapter 2, broad coverage was found to be the most common morphology, followed by LLAP, with 10,626 and 3,018 h, respectively (Fig. 18). Because broad coverage and LLAP often occurred simultaneously, and the number of hours for each occurring in isolation (i.e., with no other morphological types) was computed, along with the number of hours with both occurring simultaneously. This yielded 8,900 h of broad coverage occurring in isolation, 1291 h of LLAP in isolation, and 1726 h with both occurring simultaneously (Fig. 18). The other 5 morphology types (shoreline, lake-orographic, hybrid, MCV, and miscellaneous) were less common, with a total of 254, 226, 106, 20, and 259 h, respectively.

Diurnal behavior was analyzed specifically for broad coverage only and LLAP periods. Although neither broad coverage nor LLAP exhibit much of a diurnal signal in

the winter, LLAP exhibits a stronger diurnal signal in the fall and spring compared to LEPs in general (cf. Figs. 12, 19). During the fall, when the signal is strongest, LLAP is four times more likely during the morning peak (0800-0900 LST) than during the afternoon minimum (1500-1600 LST (Fig 19d)]. We hypothesize that the strong dependence of LLAP on land-breeze circulations (e.g., Peace and Sykes 1966; Hjelmfelt 1990; Steiger et al. 2013) contributes to this greater diurnal modulation.

The frequency of echoes $\geq$ 10 dBZ for broad coverage periods closely resembles the frequency of echoes $\geq$10 dBZ for all events, likely due to the fact that broad coverage comprises ~70% of the total hours of lake-effect observed (cf. Figs. 13a, 20a). Frequencies calculated for broad coverage and other morphological types are relative only to each type, not relative to LEPs as a whole. The analysis for LLAP periods shows the favored location for these bands, with a strip of highest frequency centered along the southern shore of Mexico Bay that broadens inland and over the Tug Hill Plateau (Fig. 20b). Although this strip may seem a bit south of that expected based on conceptual models showing convergent land breezes meeting in the center of the lake (Ladue 1996), the southern shoreline near Mexico Bay actually lies closer to the central axis of Lake Ontario as a whole. Nevertheless, further work is needed to fully elucidate the causes of the high frequency of echoes during LLAP events near Mexico Bay.

A zonal CFDD for LLAP periods illustrates some of the orographic effects over the Tug Hill during these intense events, with a very pronounced peak at all reflectivities > ~10 dBZ over the western slope near NRD. For reflectivities < ~ 10 dBZ, there is a local minimum over the western slope near NRD, suggesting precipitation is more continuous and less showery over the plateau than over the lake and coastal lowlands.

Compared with LEPs as a whole, LLAP events feature a higher frequency of the strongest reflectivities and a lower frequency of the weakest reflectivities, especially near NRD (cf., Figs. 17b, 21).

The echo frequency for shoreline periods shows a frequency maximum just offshore and parallel to the central portion of the southern shore of Lake Ontario (Fig. 20c). Precipitation features during these periods tend to form along the land-breeze front and, with weak flow, rarely penetrate more than ~10km inland, although there is a localized coastal protrusion of frequent returns southeast of Oswego (OSW).

Echoes corresponding to the lake-orographic morphology exhibit a frequency maximum centered on the plateau (Fig. 20d). The signatures from LLAP bands that accompanied some of these events are evident to the north and south of the plateau. The difference in echo frequency near the lake shore (< 30%) and over the upper plateau (> 80%) is the largest observed for any morphology type and illustrates the dramatic orographic enhancement process that can occur over the plateau.

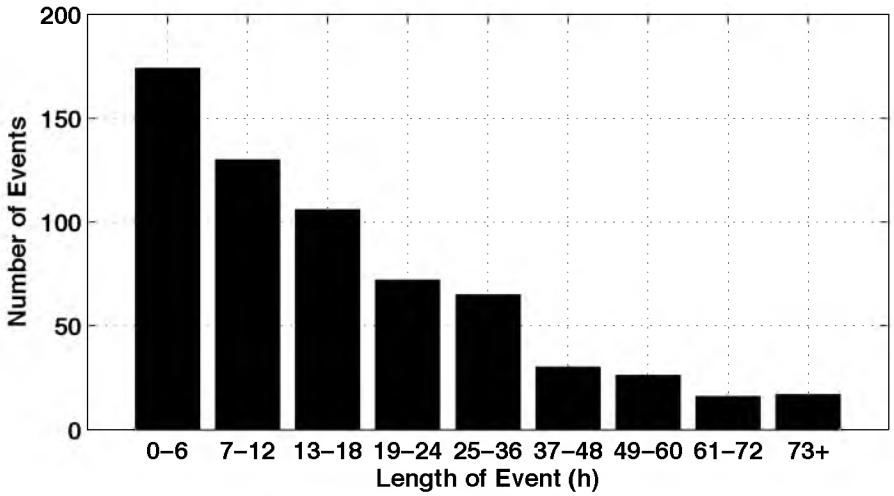

Figure 4. LEP durations.

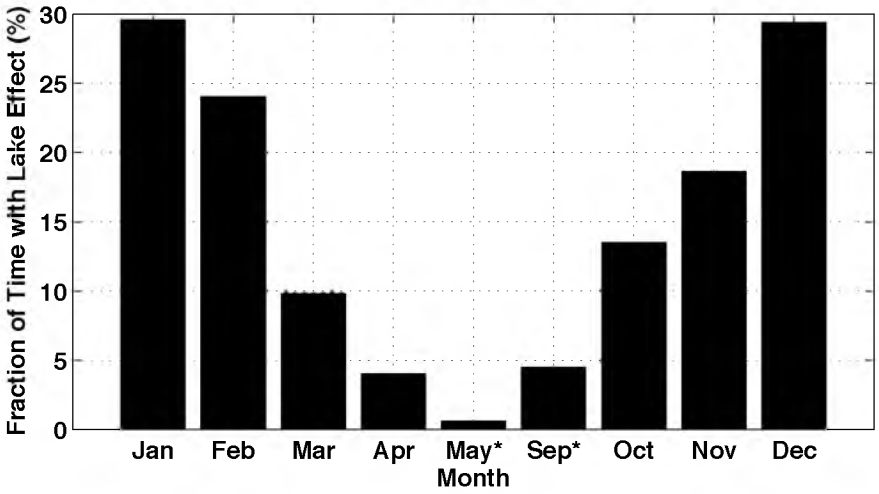

Figure 5. The fraction of time during which lake effect was observed for each month.

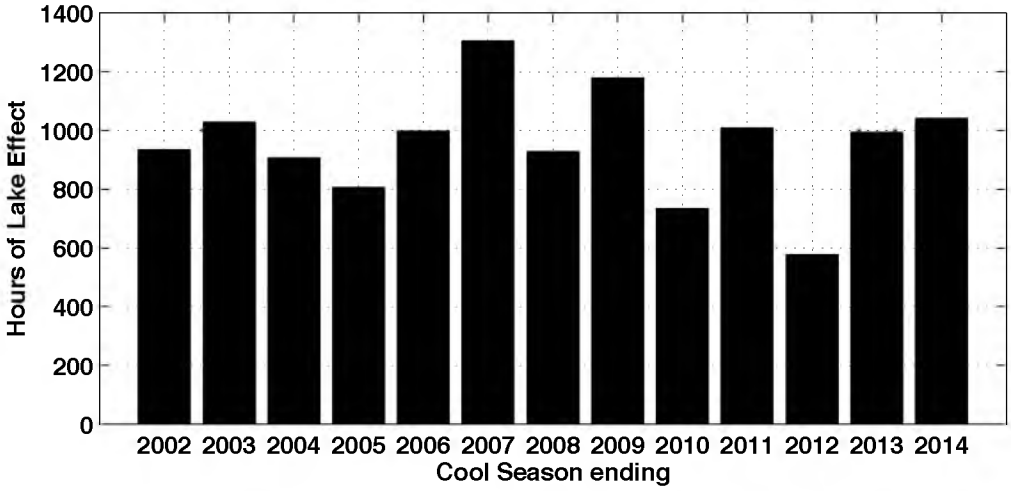

Figure 6. Hours of lake effect by cool season

Table 1. Surface observing site information. Mean cool season SWE and snowfall amounts are for the study period (2001–2014).

Identifier	Name	Elevation	Mean SWE	Mean Snow	Mean SWE LEF, Mean Snow LEF
WTN	Watertown	152 m	88 cm	304 cm	.34, .72
HKR	Hooker 12NNW	440 m	112 cm	567 cm	.42, .76
LWV	Lowville	262 m	81 cm	327 cm	.31, .67
NRD	North Redfield	399 m	N/A	718 cm	N/A, .74
BGM	Big Moose 3SE	536 m	85 cm	354 cm	.25, .61
OSW	Oswego East	107 m	84 cm	339 cm	.24, .71
BBR	Bennett's Bridge	201 m	88 cm	416 cm	.37, .70
HMK	Highmarket	537 m	111 cm	542 cm	.38, .74

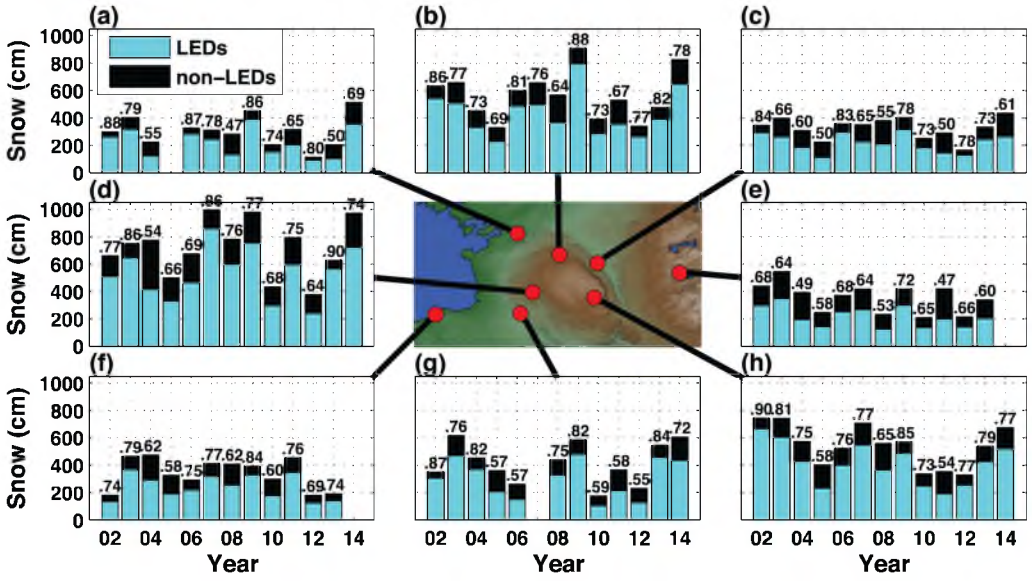

Figure 7. Total cool season snowfall during the 13-year study period at (a) WTN (b) HKR (c) LWV (d) NRD (e) BGM (f) OSW (g) BBR and (h) HMK. Fraction produced on lake-effect days indicated in light blue, with LEF annotated.

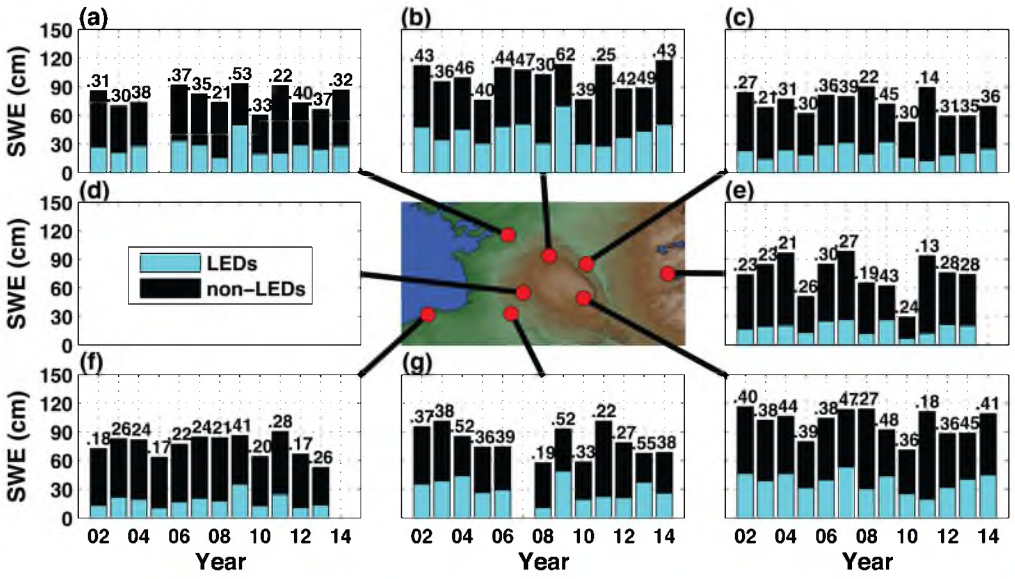

Figure 8. Same as Fig. 7, except for total cool season SWE and North Redfield not available.

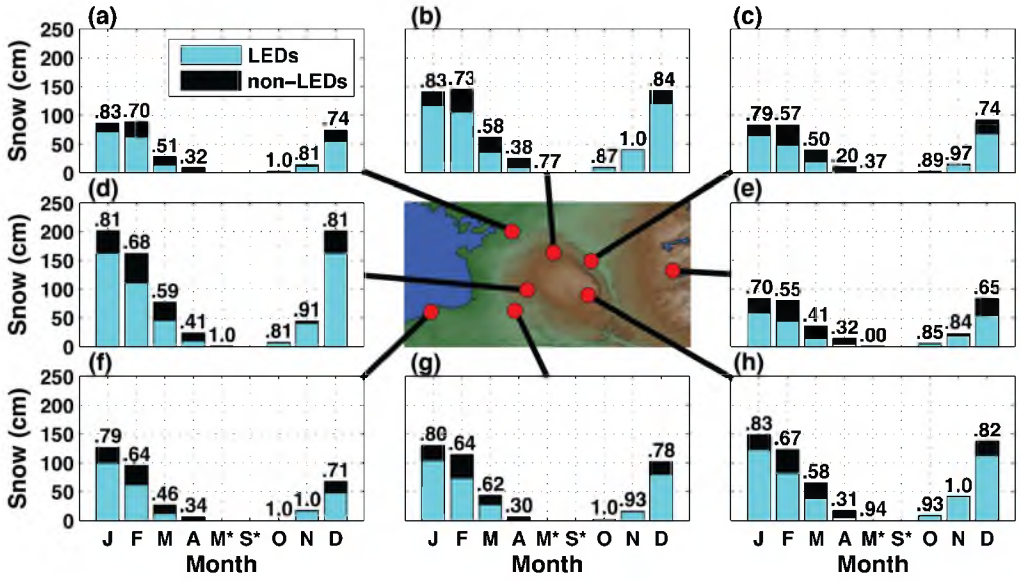

Figure 9. Same as Fig. 7, except for mean monthly snowfall. The cool season spans 16 Sep-15 May, and the * indicates that September and May include data only for the first and latter half of each month, respectively.

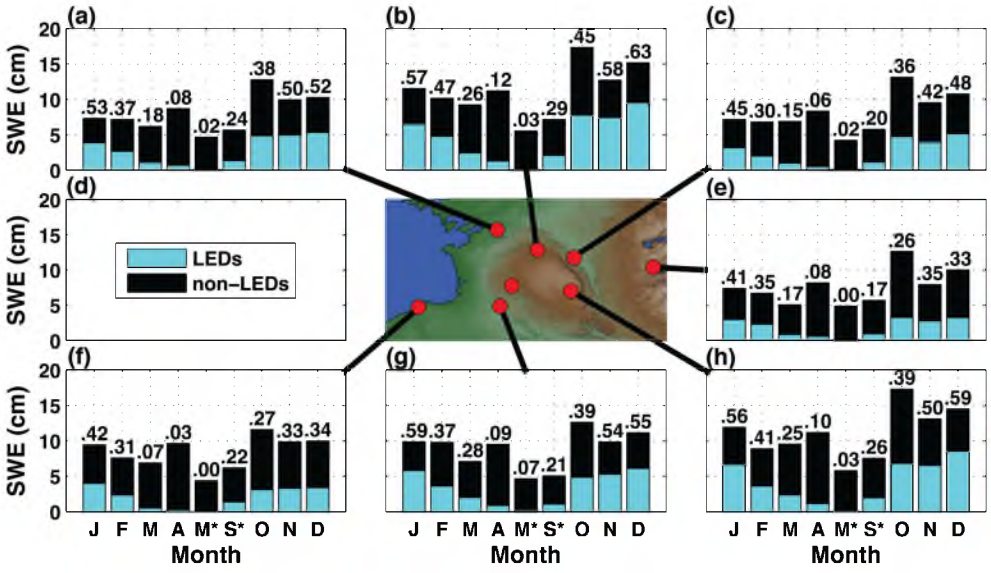

Figure 10. Same as Fig. 7, except for mean monthly SWE and North Redfield not available. The cool season spans 16 Sep-15 May, and the * indicates that September and May include data only for those days of the month.

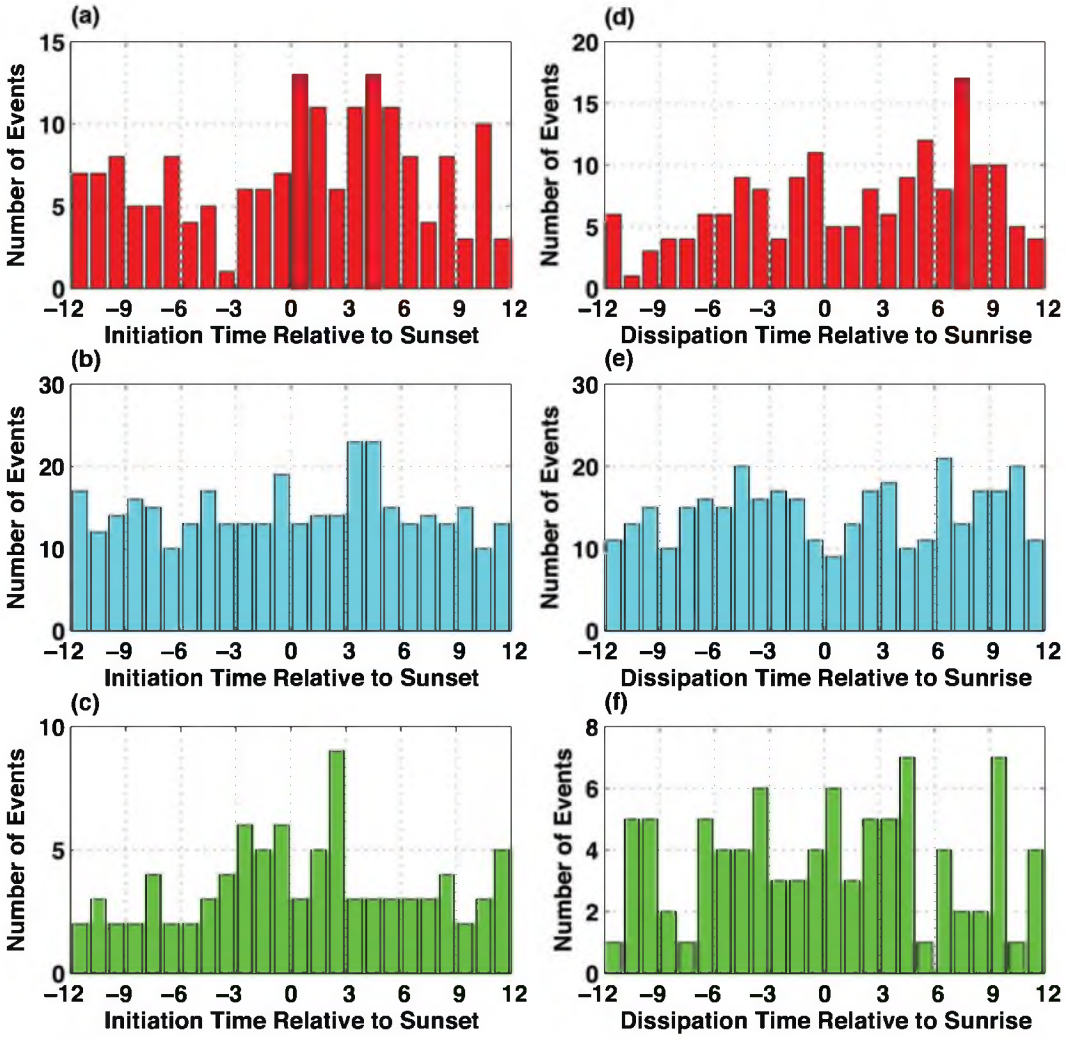

Figure 11. Initiation time of LEPs relative to sunset for (a) fall (SON) (b) winter (DJF) and (c) spring (MAM). (d-f) Same as (a-c), except for dissipation relative to sunrise.

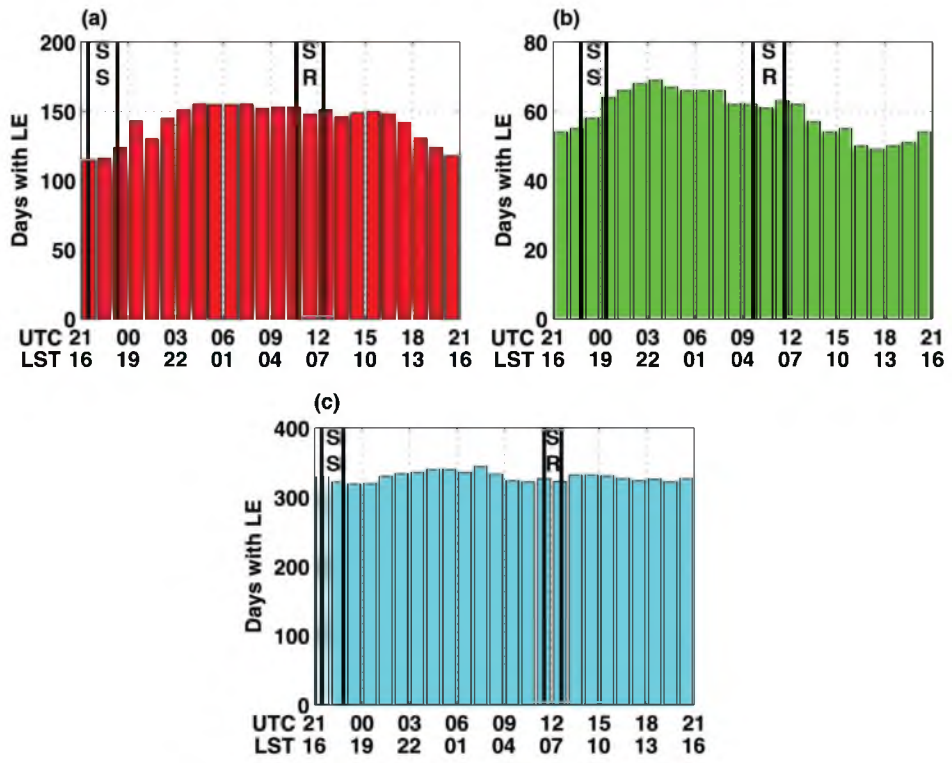

Figure 12 Number of days with lake effect observed at the specified hour of the day for (a) fall (SON) (b) spring (MAM) and (c) winter (DJF). Sunrise (SR) and sunset (SS) times are noted.

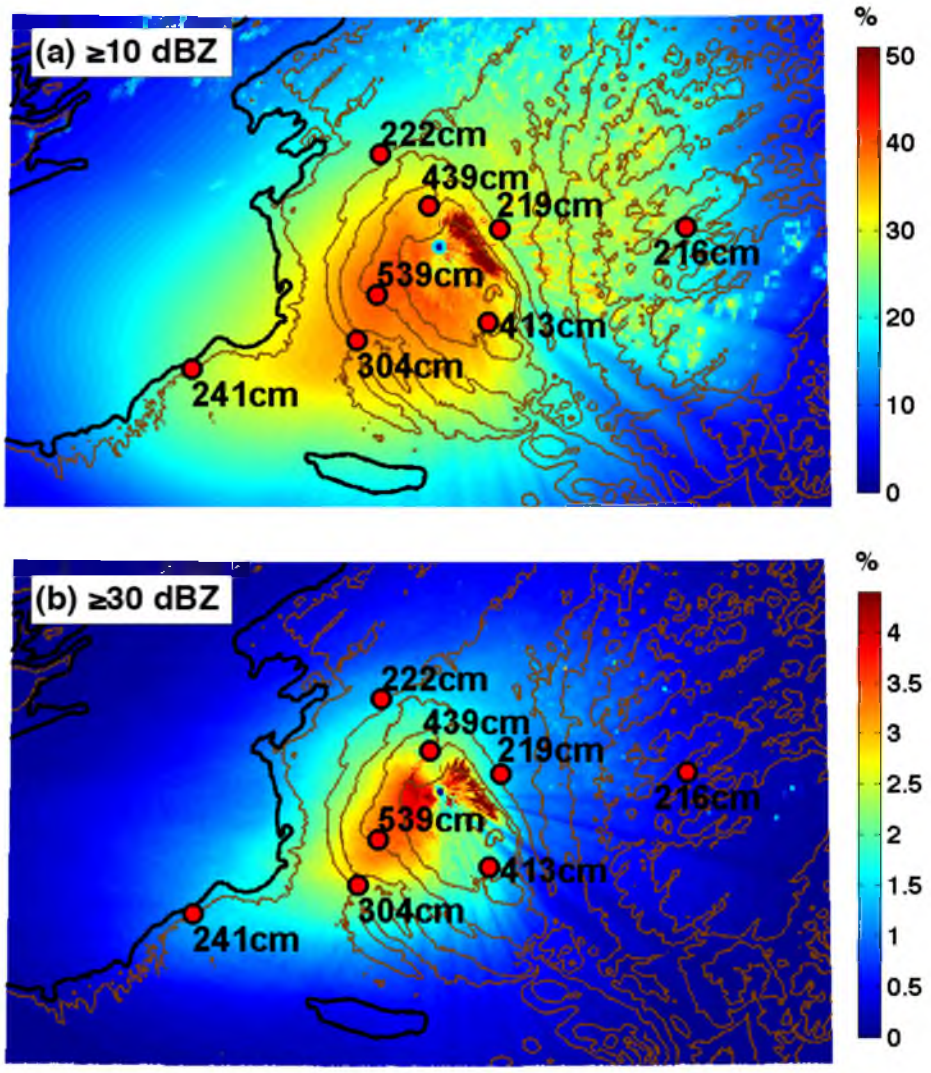

Figure 13. Frequency of echoes (a) ≥10 dBZ during LEPs, with mean (2001–2014) cool–season snowfall for LEPs from COOP sites overlaid. (b) Same as (a) except for echoes ≥30 dBZ.

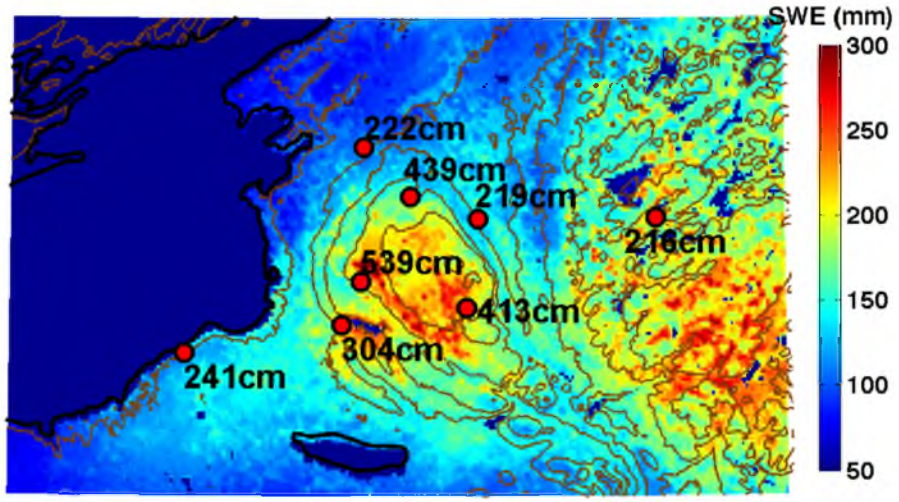

Figure 14. Mean (2003–2014) maximum snowpack water content from SNODAS with mean (2001–2014) cool-season snowfall for LEPs from COOP sites overlaid.

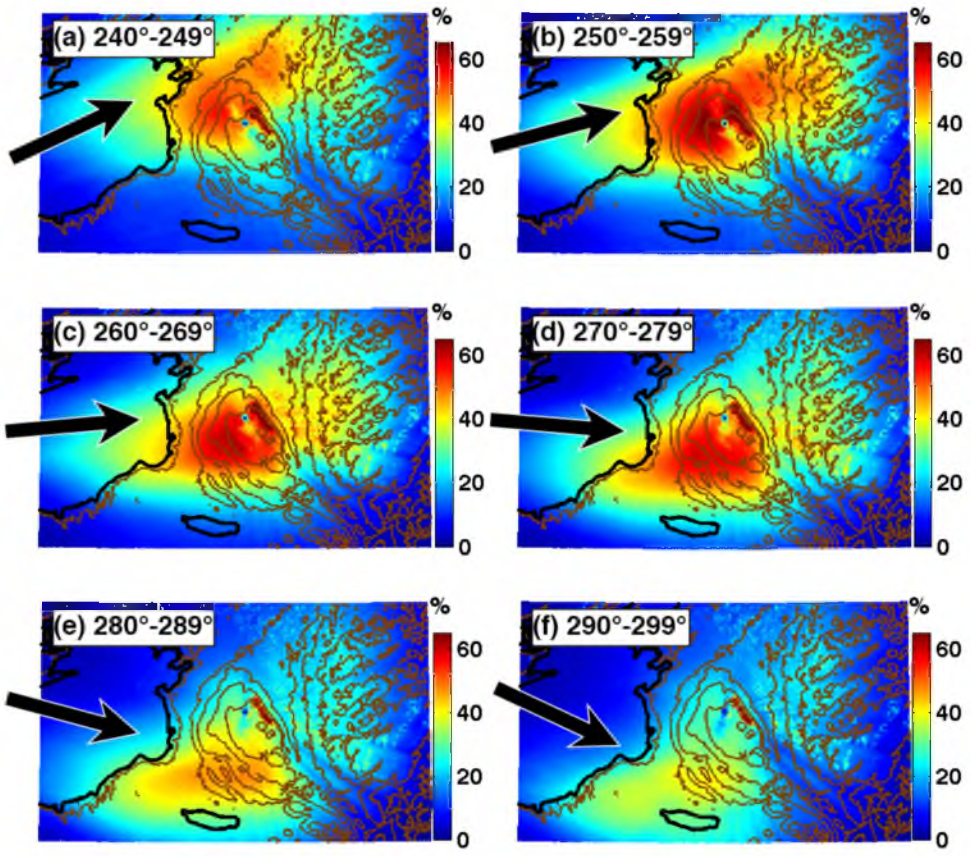

Figure 15. Frequency of echoes ≥ 10 dBZ for volume scans during which the mean 975–850 hPa wind direction is from (a) 240°–249° (b) 250°–259° (c) 260°–269° (d) 270°–279° (e) 280°–289° (f) 290°–299°. The direction of the middle value in each range is indicated by a black arrow.

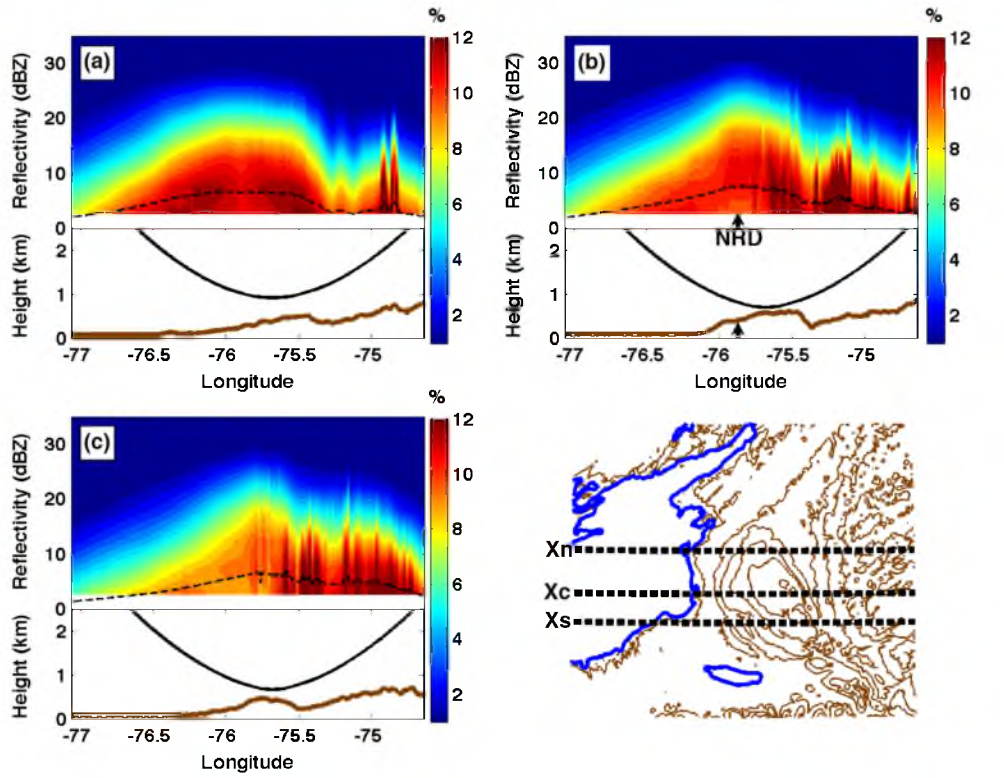

Figure 16. Contoured frequency of reflectivity by distance (CFDD) along zonal transects at (a) 43.86°N (b) 43.47°N (c) 43.63°N. The lower plot shows elevation MSL of the surface along each transect (brown) and the height of the centroid of the 0.5° beam from KTYX under standard atmospheric refraction conditions (black). The location of NRD is indicated in (b).

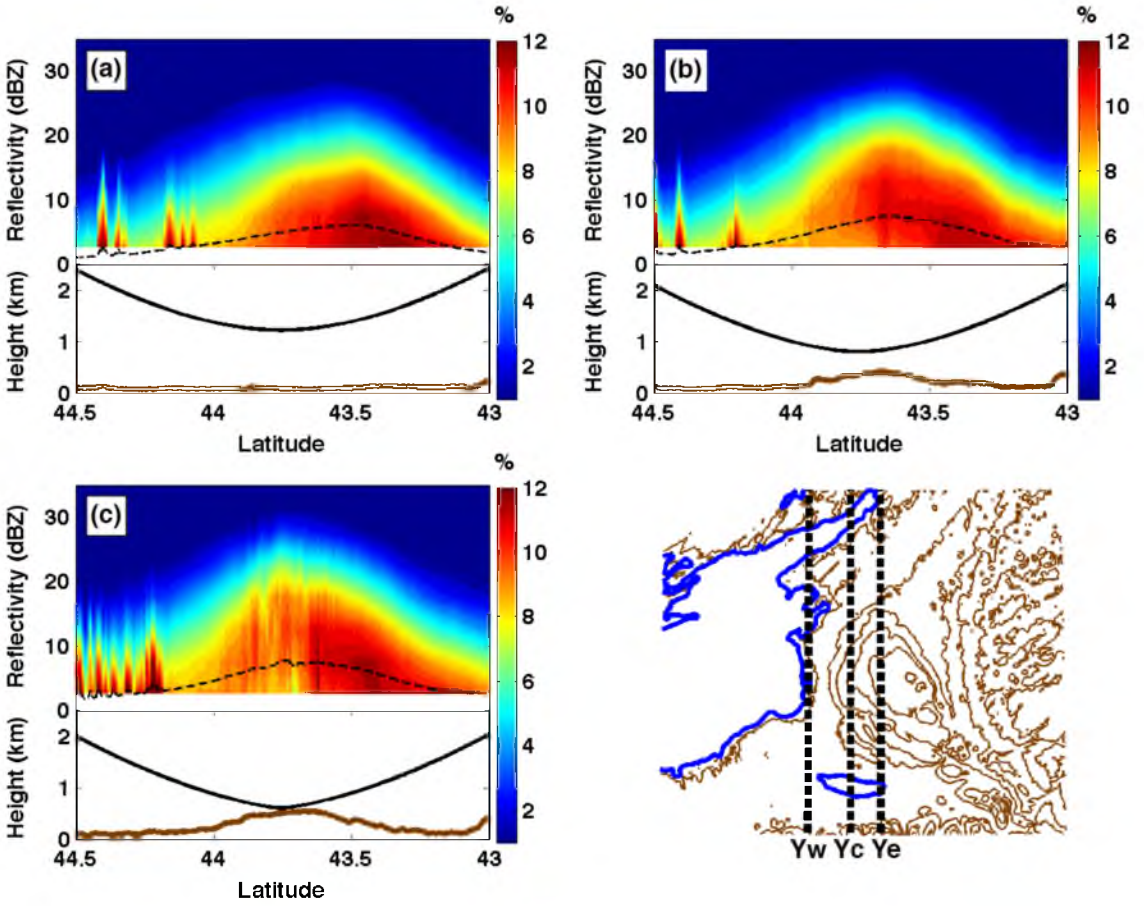

Figure 17. Contoured frequency of reflectivity by distance (CFDD) along meridional transects at (a) 76.18W (b) 75.95W (c) 75.77W. The black dashed lines indicate the mean reflectivity value. The lower plot shows elevation MSL of the surface along each transect (brown) and the height of the centroid of the 0.5° beam from KTYX under standard atmospheric refraction conditions (black).

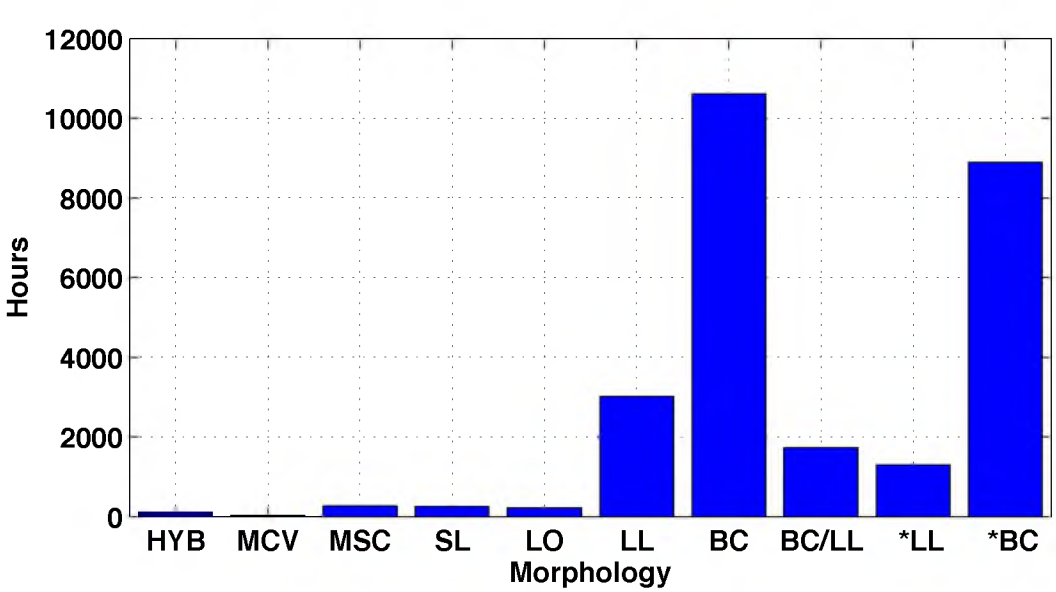

Figure 18. Hours of lake effect for hybrid (HYB), mesoscale vortex (MCV), miscellaneous (MSC), shoreline (SL), lake-orographic (LO), LLAP (LL), broad coverage (BC), BC/LL (both occurring concurrently), LLAP only (*LL), and broad coverage only (*BC).

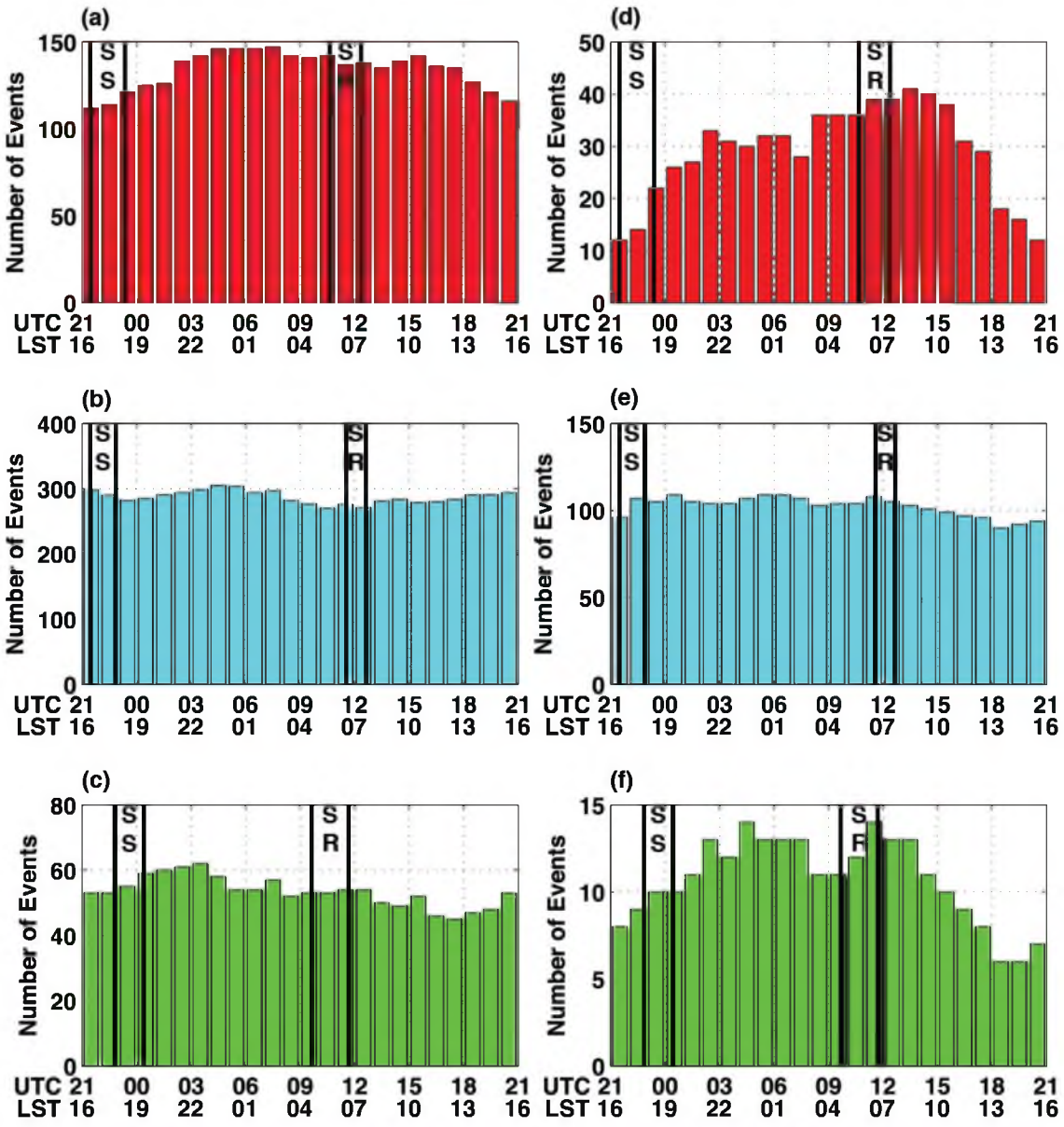

Figure 19. Same as Fig. 12, except for broad coverage events (a–c) and LLAP events (d–f)

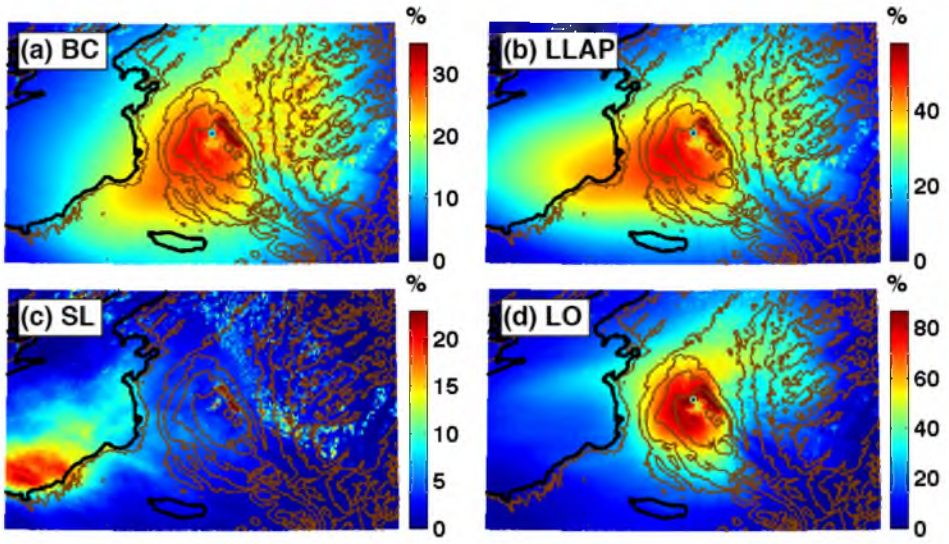

Figure 20. Frequency of echoes ≥10 dBZ during (a) broad coverage only (b) LLAP (c) shoreline and (d) lake-orographic periods.

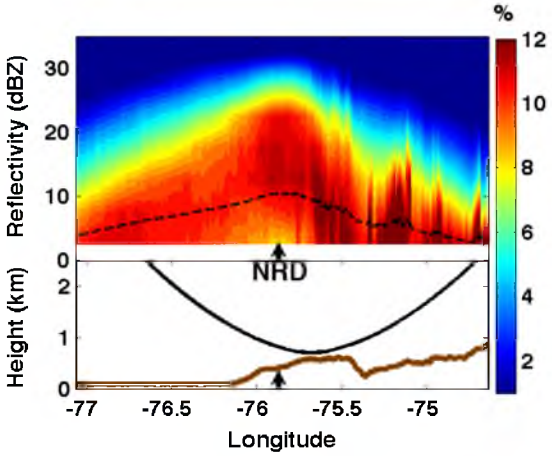

Figure 21. Cumulative frequency of reflectivity values by longitudinal distance (CFDD) along the X_c transect for LLAP periods, with location of NRD indicated.

CHAPTER 4

SUMMARY AND CONCLUSIONS

4.1 Summary of Findings

This study has presented a climatology of lake-effect precipitation east of Lake Ontario and over the Tug Hill Plateau. During the 13 cool-season (16 September – 15 May) study period (2001–2014, with the year based on the ending cool-season month), we identified 636 lake-effect periods (LEPs) in this region. Lake-effect hours totaled 12,434 (a mean of 956 per cool-season), increased through the fall to a broad maximum in December and January, and then decreased through the spring. The mean (median) LEP length was 19.5 h (13.2 h), with ~3 events per year lasting >48 h. By cool season, lake-effect hours ranged from 577 in 2012 to 1308 in 2007.

Lake effect is the dominant contributor to snowfall in the region, with a lesser, but still sizeable contribution to SWE. The fraction of monthly snowfall produced on lake-effect days peaks in the fall months (nearly all October and November snow falls on lake-effect days), whereas the fraction of monthly SWE peaks in December and January. Radar echo frequency, surface observations, and snowpack SWE data from SNODAS all suggest that the maximum lake-effect snowfall and SWE lies on the western slope or upper plateau near and east of North Redfield and intermediate to the Hooker and Highmarket COOP sites. These datasets also show a dramatic increase in snowfall, SWE, and seasonal snowpack from the coastal lowlands to the western slope and upper

plateau.

Spatial patterns of radar reflectivity frequencies during all LEPs exhibit an arm of high frequency along the southeast shore of Lake Ontario near Mexico Bay with a broadening and intensification to a maximum over the Tug Hill Plateau. Calculating echo frequency with a subdivision by 975–850 hPa mean wind direction shows that the axis of heaviest precipitation shifts south (north) when the winds gain more of a northerly (southerly) component (Fig. 15a-f), with winds from 280°-299° yielding a more modest frequency maximum than the other wind directions, which is displaced to the southern portion of the plateau, although there remains an area of elevated frequency over the northern and central portions of the plateau (Fig. 15e,f). The zonal CFDD transects depict the area of heaviest and most frequent precipitation slightly to the windward side of the crest in the central and southern portions of the plateau, with the maximum occurring almost directly over the crest in the north (Fig. 16). Although some blocked radials and scattering/signal power extinction from the Maple Ridge Wind Farm complicate the analysis, there is a decrease in frequency over the Black River Valley followed by a slight rebound over the Adirondacks for all zonal transects (Fig. 16).

A diurnal cycle of decreased (increased) lake effect occurrence in the afternoon (night/early morning) is documented, and this is in agreement with the findings of previous studies such as Kristovich and Spinar (2005) over the Great Lakes and Alcott et al. (2012) over the Great Salt Lake, although the amplitude of the signal in this study is weaker, especially compared to the Great Salt Lake. The diurnal variability for LLAP (broad coverage) events is more (less) amplified than that for LEPs in general. As with LEPs in general, both morphology types have no significant diurnal variability during the

winter.

By morphology type, broad coverage is the most common (10,626 h), followed by LLAP (3,018 h), with the other 5 types (shoreline, lake-orographic, hybrid, MCV, and Misc) considerably less common. The frequency of echoes for lake-orographic events is highest over the upper slopes on the west side and top of the plateau, with the largest increase in echo frequency from lowlands to plateau of any morphology type. The echo frequency for LLAP indicates that the central Tug Hill and the southern Lake Ontario shoreline near Mexico Bay experience the most frequent LLAP periods. CFDD analysis reveals that the increase in frequency and intensity of echoes from the coastal lowlands to plateau is lower during LLAP periods, suggesting that the increase in precipitation from coastal lowlands to plateau may also be lower (cf. Figs. 17b, 21). LLAP periods also see a greater increase in frequency of medium intensity echoes than high intensity echoes from lowlands to plateau, and the frequency of low intensity echoes actually decreases over the plateau (Fig. 21).

4.2 Conclusion and Future Work

This study has examined many of the climatological aspects of lake effect over the study area, including intraseasonal, interannual, diurnal, spatial, and morphological characteristics, and has illustrated the remarkable orographic influence of a relatively broad and modest plateau on lake-effect precipitation systems. However, further study is needed elucidate the processes behind the orographic effects observed over the Tug Hill Plateau during LEPs, including case studies of individual lake events, and examination of additional sources of data providing a truly vertical profile during lake-effect storms. Fortunately, the recently completed Ontario Winter Lake-Effect Systems (OWLeS)

project should prove immensely beneficial in providing this kind of data, and future work will utilize it.

REFERENCES

Alcott, T. I., W. J. Steenburgh, N. F. Laird, 2012: Great Salt Lake–Effect precipitation: Observed frequency, characteristics, and associated environmental factors. *Wea. Forecasting*, **27**, 954–971.

——, W. J. Steenburgh, 2013: Orographic influences on a Great Salt Lake–Effect snowstorm. *Mon. Wea. Rev.*, **141**, 2432–2450.

Baxter, M. A., C. E. Graves, and J. T. Moore, 2005: A climatology of snow-to-liquid ratio for the contiguous United States. *Wea. Forecasting*, **20**, 729–744.

Braham, R. R., 1983: The Midwest snow storm of 8–11 December 1977. *Mon. Wea. Rev.*, **111**, 253–272.

Brown, R. A., T. A. Niziol, N. R. Donaldson, P. I. Joe, V. T. Wood, 2007: Improved detection using negative elevation angles for mountaintop WSR-88Ds. Part III: Simulations of shallow convective activity over and around Lake Ontario. *Wea. Forecasting*, **22**, 839–852.

Burt, C.A., 2004: *Extreme Weather*. 2nd ed. W.W. Norton and Company, 303 pp.

Carpenter, D. M., 1993: The lake effect of the Great Salt Lake: Overview and forecast problems. Wea. Forecasting, **8**, 181– 193.

Crum, T. D., R. L. Alberty, and D. W. Burgess, 1993: Recording, archiving and using WSR-88D data. Bull Amer. Meteor. Soc., **74**, 645-653.

Dole, R. M., 1928: Snow Squalls of the Lake Region. *Mon. Wea. Rev.*, **56**, 512-513.

Forbes, G. S., J. H. Merritt, 1984: Mesoscale vortices over the Great Lakes in wintertime. *Mon. Wea. Rev.*, **112**, 377–381.

Henne, P. D., F. S. Hu, and D. T. Cleland, 2007: Lake-effect snow as the dominant control of mesic-forest distribution in Michigan, USA. *J. Ecology,* **95**, 517–529.

Hill, J. D., 1971: Snow squalls in the lee of Lakes Erie and Ontario. NOAA Tech. Memo. NWS ER-43, 20 pp.

Hjelmfelt, M. R., 1990: Numerical study of the influence of environmental conditions on

lake-effect snowstorms over Lake Michigan. *Mon. Wea. Rev.*, **118**, 138–150.

——, 1992: Orographic effects in simulated lake-effect snowstorms over Lake Michigan. *Mon. Wea. Rev.*, **120**, 373–377.

Hozumi, K., and C. Magono, 1984: The cloud structure of convergent cloud bands over the Japan Sea in winter monsoon period. *J. Meteor. Soc. Japan*, **62**, 522–533.

Kelly, R. D., 1982: A single Doppler radar study of horizontal-roll convection in a lake-effect snow storm. *J. Atmos. Sci.*, **39**, 1521–1531.

——, 1984: Horizontal roll and boundary-layer interrelationships observed over Lake Michigan. *J. Atmos. Sci.*, **41**, 1816–1826.

——, 1986: Mesoscale frequencies and seasonal snowfalls for different types of Lake Michigan snow storms. *J. Climate Appl. Meteor.*, **25**, 308–312.

Kindap, T., 2010: A severe sea-effect snow episode over the city of Istanbul. *Nat. Hazards*, **54**, 707–723.

Kristovich, D. A. R., 1993: Mean circulations of boundary-layer rolls in lake-effect snow storms. *Bound.-Layer Meteor.*, **63**, 293–315.

——, M. L. Spinar, 2005: Diurnal variations in lake-effect precipitation near the western Great Lakes. *J. Hydrometeor*, **6**, 210–218.

Laird, N. F., 1999: Observation of coexisting mesoscale lake-effect vortices over the western Great Lakes. *Mon. Wea. Rev.*, **127**, 1137–1141.

——, D. A. R. Kristovich, 2004: Comparison of observations with idealized model results for a method to resolve winter lake-effect mesoscale morphology. *Mon. Wea. Rev.*, **132**, 1093–1103.

——, J. Desrochers, and M. Payer, 2009a: Climatology of lake- effect precipitation events over Lake Champlain. *J. Appl. Meteor. Climatol.*, **48**, 232–250.

LaDue, J., 1996: COMET course notes and satellite meteorology

Leffler, R. J., R. M. Downs, G. W. Goodge, N. J. Doesken, K. L. Eggleston, and D. Robinson, 1997: Evaluation of the Reported January 11-12, 1997, Montague, New York, 77-inch, 24-Hour Lake-Effect Snowfall. National Weather Service Special Report. 60 pp, http://www1.ncdc.noaa.gov/pub/data/cmb/extremes/ncec/mantague-ny-snowfall-24hour.pdf

Magono, C., K. Kikuchi, T. Kimura, S. Tazawa, and T. Kasai, 1966: A study on the snowfall in the winter monsoon season in Hokkaido with special reference to low

land snowfall. *J. Fac. Sci. Hokkaido Univ. Ser.* **7**, 11, 287–308.

Matsuura, S., K. Matsuyama, S. Asano, T. Okamoto, and Y. Takeuchi, 2005: Fluctuation of the seasonal snowpack in a mountainous area of the heavy-snow district in the warm- temperate zone of Japan. *J. Glaciol.*, **51**, 547–554.

Mesinger, F., and Coauthors, 2006: North American Regional Reanalysis. *Bull. Amer. Meteor. Soc.*, **87**, 343–360.

Miner, T. J., and J. M. Fritsch, 1997: Lake-effect rain events. *Mon. Wea. Rev.*, **125**, 3231–3248.

Muller, R.A., 1966: Snowbelts of the Great Lakes. *Weatherwise*, **19**, 248-255

National Operational Hydrologic Remote Sensing Center. 2004. *Snow Data Assimilation System (SNODAS) Data Products at NSIDC.* Snowpack Snow-Water Equivalent. Boulder, Colorado USA: National Snow and Ice Data Center.

National Weather Service Forecast Office Burlington, VT, cited 2014: National Weather Service WSR-88D Radar and Wind Farm Impacts. [Available online at http://www.erh.noaa.gov/btv/research/Wind_Farm/]

National Weather Service Forecast Office Buffalo, NY, cited 2014: Summary of Lake-Effect Snow Event over the Tug Hill February 3-12, 2007. [Available online at http://www.erh.noaa.gov/buf/locust/]

Niziol, T. A., W. R. Snyder, J. S. Waldstreicher, 1995: Winter weather forecasting throughout the eastern United States. Part IV: Lake effect snow. *Wea. Forecasting*, **10**, 61–77.

Norton, D.C., and S.J. Bolsenga, 1993: Spatiotemporal trends in lake-effect and continental snowfall in the Laurentian Great Lakes, 1951-1980. *J. Clim.*, **6**, 1943-1956.

Onton, D. J., and W. J. Steenburgh, 2001: Diagnostic and sensitivity studies of the 7 December 1998 Great Salt Lake–effect snowstorm. *Mon. Wea. Rev.*, **129**, 1318–1338.

Passarelli, R. E., R. R. Braham, 1981: The role of the winter land breeze in the formation of Great Lake snow storms. *Bull. Amer. Meteor. Soc.*, **62**, 482–492.

Peace, R. L., and R. B. Sykes, 1966: Mesoscale study of a lake effect snow storm. *Mon. Wea. Rev.*, **94**, 495–507.

Rodriguez, Y., D. A. R. Kristovich, and M. R. Hjelmfelt, 2007: Lake-to-lake cloud bands: Frequencies and locations. *Mon. Wea. Rev.*, **135**, 4202–4213.

Steenburgh, W. J., S. F. Halvorson, and D. J. Onton, 2000: Climatology of lake-effect snowstorms of the Great Salt Lake. *Mon. Wea. Rev.*, **128**, 709–727.

——, and D. J. Onton, 2001: Multiscale analysis of the 7 December 1998 Great Salt Lake–effect snowstorm. *Mon. Wea. Rev.*, **129**, 1296–1317.

——, 2003: One hundred inches in one hundred hours: Evolution of a Wasatch Mountain winter storm cycle. *Wea. Forecasting*, **18**, 1018–1036.

——, 2014: *Secrets of the Greatest Snow on Earth*. Utah State University press, 244 pp.

Steiger, S. M., and Coauthors, 2013: Circulations, bounded weak echo regions, and horizontal vortices observed within long-lake-axis-parallel–lake-effect storms by the Doppler on Wheels. *Mon. Wea. Rev.*, **141**, 2821–2840.

Radar Operations Center, 2009: Wind Farms: Coming Soon to a WSR-88D Near You. [Available online at http://www.roc.noaa.gov/WSR88D/NNOW/NNowContent.aspx?Topic=WindFarmSoon]

Tug Hill Commission, cited 2014: Environment and Economy. [Available online at http://www.tughill.org/environment-economy/]

Wilks, D. S. 2006: *Statistical Methods in the Atmospheric Sciences*. 2nd ed. Elsevier, 627 pp.

Yeager, K. N., W. J. Steenburgh, and T. I. Alcott, 2013: Contributions of lake-effect periods to the cool-season hydroclimate of the Great Salt Lake basin. *J. Appl. Meteor. Climatol.*, **52**, 341–362.